Polyethylene-Glycol-Modified Single-Walled Carbon Nanotubes for Intra-Articular Delivery to Chondrocytes

Cristiano Sacchetti,[†,‡] Ru Liu-Bryan,[§] Andrea Magrini,[∥] Nicola Rosato,[⊥] Nunzio Bottini,[*,‡] and Massimo Bottini[*,†,‡,⊥]

[†]Inflammatory and Infectious Disease Center, Sanford Burnham Medical Research Institute, La Jolla, California 92037, United States, [‡]Division of Cellular Biology, La Jolla Institute for Allergy and Immunology, La Jolla, California 92037, United States, [§]Department of Medicine, VA Medical Center, University of California San Diego, San Diego, California 92093, United States, and [∥]Department of Biopathology and Imaging Diagnostics and [⊥]Department of Experimental Medicine and Surgery, University of Rome Tor Vergata, Rome 00173, Italy

ABSTRACT Osteoarthritis (OA) is a common and debilitating degenerative disease of articular joints for which no disease-modifying medical therapy is currently available. Inefficient delivery of pharmacologic agents into cartilage-resident chondrocytes after systemic administration has been a limitation to the development of anti-OA medications. Direct intra-articular injection enables delivery of high concentrations of agents in close proximity to chondrocytes; however, the efficacy of this approach is limited by the fast clearance of small molecules and biomacromolecules after injection into the synovial cavity. Coupling of pharmacologic agents with drug delivery systems able to enhance their residence time and cartilage penetration can enhance the effectiveness of intra-articularly injected anti-OA medications. Herein we describe an efficient intra-articular delivery nanosystem based on single-walled carbon nanotubes (SWCNTs) modified with polyethylene glycol (PEG) chains (PEG-SWCNTs). We show that PEG-SWCNTs are capable to persist in the joint cavity for a prolonged time, enter the cartilage matrix, and deliver gene inhibitors into chondrocytes of both healthy and OA mice. PEG-SWCNT nanoparticles did not elicit systemic or local side effects. Our data suggest that PEG-SWCNTs represent a biocompatible and effective nanocarrier for intra-articular delivery of agents to chondrocytes.

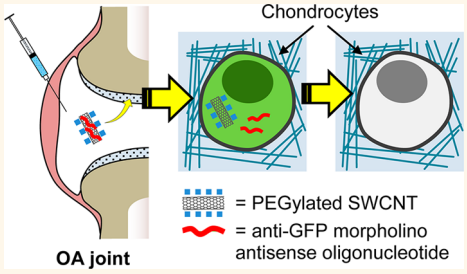

KEYWORDS: osteoarthritis · chondrocytes · intra-articular injection · carbon nanotubes · morpholino antisense oligonucleotides · gene inhibition · confocal microscopy

Osteoarthritis (OA) is a common degenerative disease of the articular joints, which affects up to a third of subjects after the age of 60.[1,2] Joint replacement surgery is commonly performed once OA has reached advanced stages; however, there currently is no medical therapy able to slow down or halt progression of disease (so-called disease-modifying OA drugs, DMOADs).[3] This makes OA one of the largest unmet medical need in the field of rheumatology. Although OA is currently viewed as a disease of the whole joint, an imbalance between the matrix-producing and matrix-degrading properties of cartilage-resident chondrocytes, especially chondrocytes residing in the superficial zone of the cartilage, plays a major pathogenic role.[4,5] Genetic manipulations in experimental animals have led to the identification of several chondrocyte molecular targets for new DMOADs able to prevent or halt progression of OA.[6−8] Unfortunately, the peculiar physiology of the joint complicates delivery of candidate therapeutic agents into chondrocytes. Since cartilage lacks significant vascular supply, delivery of systemically administered (SA) medication to chondrocytes is subordinated to their diffusion into the synovial fluid. Intra-articular (IA) administration can deliver high concentrations of therapeutic agents in close proximity to the chondrocytes.[9] However, IA-injected small molecules and biomacromolecules are quickly cleared through the lymphatic system, which often limits their residence within the synovial cavity to just a few hours.[10−12] Due to the invasive nature of IA injections,

* Address correspondence to nunzio@lji.org, mbottini@sanfordburnham.org.

Received for review August 13, 2014 and accepted November 21, 2014.

Published online November 21, 2014
10.1021/nn504537b

Scheme 1. PEG-SWCNTs as Chondrocyte-Specific Drug Delivery Systems[a]

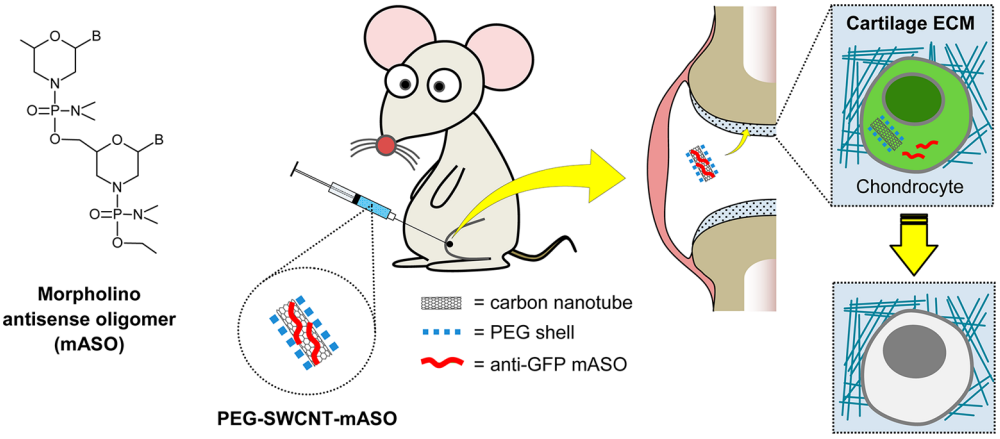

[a] Morpholino antisense oligomers (mASOs) are composed by about 25 morpholine rings carrying a nitrogenous base (B) and connected through uncharged phosphoroamidate linkages. Depending on the base sequence, mASOs block gene expression *via* diverse mechanisms. We used a mASO against a green fluorescence protein (GFP), which elicits reduction of gene expression by blocking ribosomal translation in the cytosol. Single-walled carbon nanotubes (SWCNTs) modified with polyethylene glycol (PEG) chains (PEG-SWCNTs) were loaded with anti-GFP mASOs, likely *via* π-stacking of nitrogenous bases onto the exposed (non-PEGylated) portions of nanotubes' sidewalls (PEG-SWCNT-mASO), and intra-articularly (IA) injected into the knees of both healthy and arthritic GFP transgenic mice. The particles exhibited long persistence time into the joint, entered the cartilage matrix and delivered mASOs into the cytoplasm of chondrocytes, thus eliciting a decrease in GFP expression. Since mASOs are nonpolar and their charge is unaffected by lysosomal pH, we hypothesized that the release of mASOs from PEG-SWCNTs occurs in the cytoplasm triggered by the complementarity between target mRNA and mASO.

IA-delivered DMOADs need to display persistence times of weeks, if not months, after one or few injections in order to be a clinically viable therapeutic option.[13]

An option to increase the IA persistence of therapeutic agents is to couple them to nanotech-derived drug delivery systems (DDSs).[14] However, delivery of large macromolecules to chondrocytes also has known limitations. Chondrocytes are the sole residing cells within the cartilage extracellular matrix (ECM), which is a negatively charged 3D meshwork enriched in hyaluronic acid (HA) with a pore size of ~60 nm.[15] Penetration of particles into the cartilage ECM depends on their physicochemical properties, including shape, size, surface charge, and aggregation state.[16,17] In a recent report, positively charged 38-nm-in-diameter spherical nanoparticles could enter cartilage, whereas particles with a diameter of 96 nm did not. The IA persistence of these particles was not assessed.[16]

Here we assessed the efficacy of polyethylene glycol (PEG) chain-modified single-walled carbon nanotubes (PEG-SWCNTs) as DDSs for delivery of IA agents to chondrocytes. PEG-SWCNTs are 1D nanoparticles with diameters smaller than 10 nm and lengths ranging from few tens to several hundreds of nanometers.[18] Due to their 1D structure, PEG-SWCNTs display good pharmacokinetic profiles in dense fluids/tissues and can deliver large and highly diversified drug payloads. PEG-SWCNTs readily penetrate a large variety of cells, and display excellent biocompatibility properties.[19−21] Long-term accumulation of PEG-SWCNTs into Kupffer cells following systemic administration of high doses of PEG-SWCNTs did not lead to significant liver stress or other evident systemic toxicity.[22] Additionally, we recently investigated the pattern of plasma proteins (the "blood" protein corona) adsorbed onto PEG-SWCNTs following incubation with human plasma and found that HA-binding proteins such as α-1 microglobulin were significantly enriched in the PEG-SWCNTs' protein corona.[23] Thus, the physicochemical properties and surface presentation of HA-binding proteins might confer PEG-SWCNTs the ability to penetrate and navigate the dense cartilage meshwork and deliver cargo into chondrocytes.

In this study, we investigated the joint trafficking and cartilage penetration of IA-injected PEG-SWCNTs (IA-PEG-SWCNTs). We show that IA-PEG-SWCNTs display long residence time within the joint cavity of both healthy and OA mice, and efficiently enter chondrocytes residing in the upper zone of the cartilage. IA-PEG-SWCNTs did not accumulate into major organs and did not elicit systemic or regional side effects. Importantly, IA-PEG-SWCNTs were able to deliver anti-green fluorescent protein (GFP) "third generation" morpholino antisense oligonucleotides (GFP-mASOs) into chondrocytes of healthy and arthritic GFP-transgenic mice (Scheme 1).

RESULTS

Fabrication and Characterization of PEG-SWCNT-mASOs. Amino-functionalized PEG-SWCNTs were fabricated by adsorption of phospholipids functionalized with amino-terminated 2 kDa molecular weight (MW) linear PEG chains onto pristine (nonfunctionalized) SWCNTs

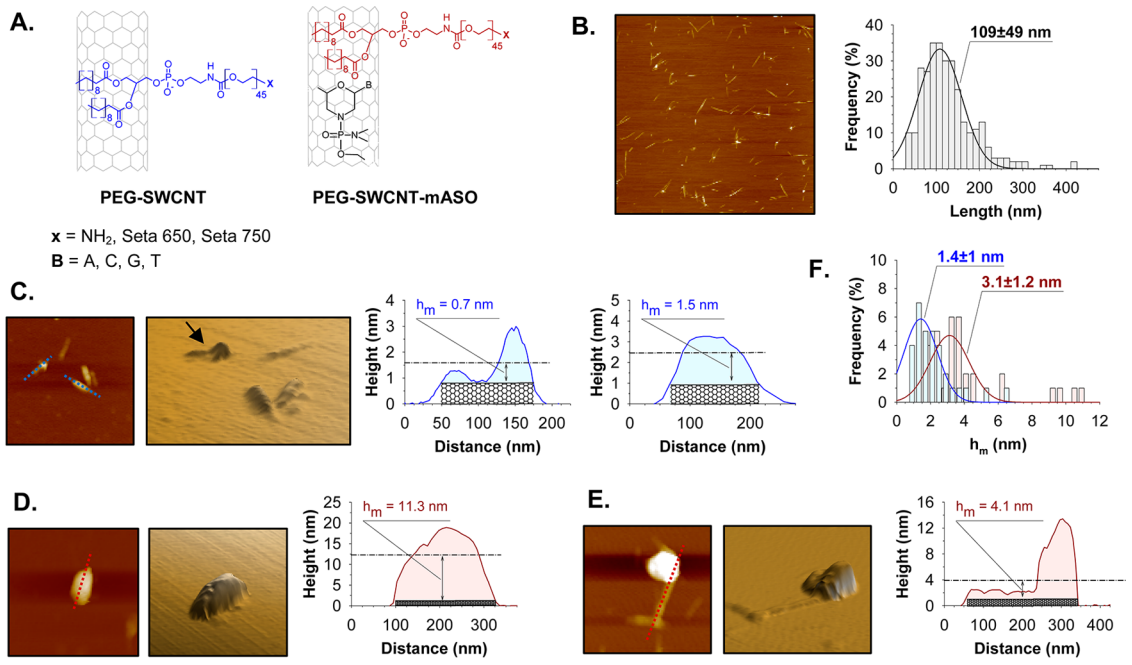

Figure 1. PEG-SWCNTs used to deliver mASOs into chondrocytes. (A) Amino-functionalized PEG-SWCNTs were obtained by coating the sidewalls of pristine (nonfunctionalized) SWCNTs with phospholipids modified with amino-terminated PEG chains. Fluorochrome-conjugated PEG-SWCNTs (PEG-SWCNT-650 or PEG-SWCNT-750) were fabricated by capping PEG terminal amino groups on amino-functionalized PEG-SWCNTs with either 650 or 750 nm emitting fluorochromes, whereas PEG-SWCNTs loaded with mASOs (PEG-SWCNT-mASOs) were obtained by adsorption of mASO molecules onto PEG-SWCNT-650. (B) AFM (topography) image (scan size 2 × 2 μm^2) and length distributions for amino-functionalized PEG-SWCNTs. (C−E) AFM images (topography), 3D-reconstructions, longitudinal cross sections, and values for the average height of PEG shell (h_m) for representative amino-functionalized PEG-SWCNTs (C) and PEG-SWCNT-mASOs (D and E). Black arrow indicates the portion of SWCNT sidewall that was exposed because it was devoid of PEG coverage. (F) Distribution of average heights of PEG shell (h_m) for amino-functionalized PEG-SWCNTs (cyan histogram) and PEG-SWCNT-mASOs (pink histogram). Mean values of h_m are reported. Scan size: 800 × 800 nm^2 (C), 700 × 700 nm^2 (D), and 500 × 500 nm^2 (E).

followed by capping the terminal amino groups with either 650 or 750 nm emitting fluorochromes (PEG-SWCNT-650 or PEG-SWCNT-750, respectively) (Figure 1A).[21] Fluorochrome-conjugated PEG-SWCNTs had a surface charge (in PBS) of −11 mV and PEG density of ∼0.1 mmol per gram of carbon material, and were sterile, free of metallic impurities, and stably dispersed in high saline solutions and culture media for several days at 37 °C without exhibiting any sign of precipitation (data not shown, and refs 23 and 24). Next, PEG-SWCNT-mASOs were fabricated by incubating PEG-SWCNT-650 with GFP-mASOs (targeting mASO, sequence: 5′-acagctcctcgcccttgctcaccat-3′) in PBS overnight (o/n) at 4 °C and subsequent washing in PBS to remove free oligos. Control nanoparticles (PEG-SWCNT-Ctr) were obtained by adsorbing nontargeting mASOs (control mASO, sequence: 5′-ggtggattgccttttcagctt-3′) onto PEG-SWCNT-650. PEG-SWCNT-mASOs were stable in high saline solutions without any detectable mASO release over hours. We calculated that approximately 50 mASO molecules adsorbed onto each PEG-SWCNT particle.

Atomic force microscopy (AFM) was used to investigate the morphology of (amino-functionalized) PEG-SWCNTs and PEG-SWCNT-mASOs. AFM images showed that PEG-SWCNTs were composed by individual needlelike particles with a narrow length distribution centered at ∼110 nm (Figure 1B). AFM longitudinal cross sections of PEG-SWCNTs were not uniform and showed peaks having a height of few nanometers. Moreover, the cross section of ∼50% of the nanoparticles in each field of view displayed flat valleys, which had a height of ∼1 nm and extended for several tens of nanometers (arrow in Figure 1C). Since the nominal (supplier-given) diameter of the employed SWCNTs was ∼1.4 nm, we interpreted the flat valleys as segments of nanotube sidewall exposed because they were devoid of PEG coverage. Whereas the PEG-SWCNT-mASOs' AFM longitudinal sections were also not uniform, they showed peaks having a maximum height up to 20 nm (Figure 1D) and valleys having a minimum height of ∼2 nm (Figure 1E). These results confirmed that mASO molecules adsorbed onto PEG-SWCNTs and suggested that the conformation of PEG chains changed following mASO adsorption onto PEG-SWCNTs.

In order to qualitatively study the conformation of PEG chains carried by PEG-SWCNTs and PEG-SWCNT-mASOs, we applied an approach we have recently developed based on the measurement of the average height (h_m) of the polymer shell decorating the nanotubes' sidewalls.[23] The value of h_m was calculated by dividing the net area of the polymer shell for the length

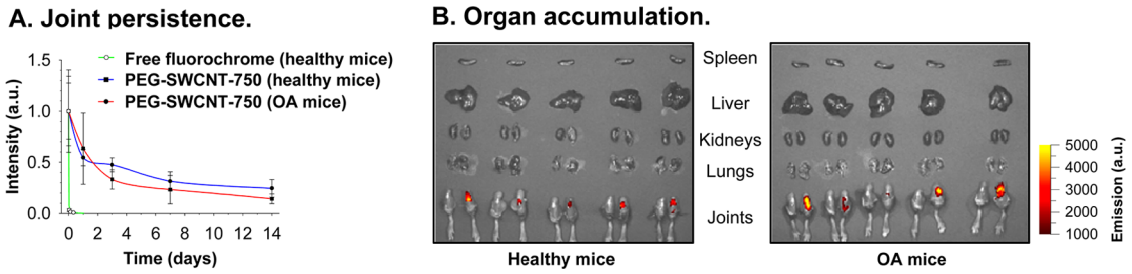

Figure 2. Joint persistence and organ accumulation of IA-injected PEG-SWCNTs. Two groups (N = 5) of healthy 3-month-old female C57BL/6J (B6) mice were unilaterally IA-injected in the knee with 5 μg of PEG-SWCNT-750 in 10 μL of PBS or equivalent doses (~0.4 μmol) of free Seta750. PEG-SWCNT-750 were also IA-injected in the arthritic knees of a group (N = 5) of 3-month-old female B6 mice with OA (1 month post-DMM surgery). NIR fluorescence images of animals were taken through the IVIS Spectrum system during the following 14 days, and the fluorescence intensity of the treated knees was measured (A). After 14 days, PEG-SWCNT-treated mice were sacrificed, the major organs (spleen, liver, kidneys, and lungs) extracted, and their NIR-emission measured. NIR signals from these organs were undetectable. Legs were also collected, the skin removed, and their NIR-emission measured. Bright NIR signals arose from treated knees (right), whereas NIR signals from untreated knees were undetectable (left) (B).

of the underneath SWCNT. The net area of the polymer shell was calculated by subtracting the area of the underneath SWCNTs from the area under the AFM longitudinal cross section curve (cyan areas in Figure 1C and pink areas in Figure 1D and E). We recorded the AFM longitudinal cross section curves for N = 35 PEG-SWCNTs and an equal number of PEG-SWCNT-mASOs, and the values of h_m were calculated. An average value of $h_m = 1.4 \pm 1$ nm and 3.1 ± 1.2 nm was found for PEG-SWCNTs and PEG-SWCNT-mASOs, respectively (Figure 1F). We have previously described that SWCNTs decorated with 2 kDa MW linear PEG chains in mushroom conformation had $h_m \sim 1$ nm, whereas particles with PEG chains in brush configuration had $h_m \geq 11$ nm, thus suggesting that PEG chains mostly laid on the nanotubes' sidewalls in a mushroom conformation for PEG-SWCNTs and, following mASO adsorption, PEG chains acquired a mushroom−brush transition conformation.[23]

IA-Injected PEG-SWCNTs Display Long Residence Time in Murine Joints. Since slow clearance from the synovial cavity is an important requisite to ensure delivery into chondrocytes of IA-injected DDSs, we first assessed whether IA-PEG-SWCNTs were able to persist in the joint cavity for a prolonged interval of time.

Two groups (N = 5) of healthy 3-month-old C57BL/6J (B6) mice were unilaterally IA-injected in the knee with PEG-SWCNT-750 (IA-PEG-SWCNT-750) or free fluorochromes (IA-Seta750). Mice were imaged through an IVIS Spectrum Preclinical *In Vivo* Imaging System during the following 14 days, and the fluorescence intensity of injected knees was measured. While the knees treated with IA-Seta750 lost the signal in less than 8 h (Figure 2A and Supporting Information Figure S1A), those treated with IA-PEG-SWCNT-750 still displayed a bright signal after 14 days (Figure 2B). Approximately 50% of IA-PEG-SWCNT-750 exited the joints within 48 h, after which the particles exhibited a distribution balance between blood and tissues for ~24 h and were eliminated very slowly from the joints. More than 25% of the starting nanoparticle fluorescence was still detectable in the joint after 2 weeks (Figure 2A).

Since inflammation and angiogenesis are involved in OA pathogenesis and may increase the speed of egression of cargo-loaded DDSs from the synovial cavity, we also investigated the residence time of IA-PEG-SWCNT-750 in OA knees.[25] OA was induced in a group (N = 5) of 2-month-old B6 mice by destabilization of the medial meniscus (DMM) through sectioning of the anteromedial meniscotibial and medial collateral ligaments in the left knee.[26] We chose the DMM as OA mouse model because it elicits mild/moderate OA over several months. One month after surgery, when the mice had developed OA (data not shown and ref 26), mice were treated with IA-PEG-SWCNT-750 in the OA knee and the NIR fluorescence of injected knees was followed through the IVIS Spectrum system. The NIR fluorescence of injected OA knees did not significantly differ from that of injected healthy joints at any of the observation time points (Figure 2A). We concluded that the pathology induced by OA did not significantly affect the distribution profile of IA-PEG-SWCNTs within the joints.

We next investigated if egression from the injected joints leads to accumulation of IA-PEG-SWCNTs into major organs and/or alterations of liver function. The NIR fluorescence exhibited by spleen, liver, kidneys, and lungs extracted from mice 14 days after unilateral treatment of joints with IA-PEG-SWCNT-750 was undetectable by the IVIS Spectrum system (Figure 2B). Serum levels of aspartate aminotransferase (AST) and alanine aminotransferase (ALT) 14 days after unilateral treatment of joints with IA-PEG-SWCNT-750 did not statistically differ from those of untreated mice (Supporting Information, Figure S1B). Additionally, creatinine exhibited not statistically different levels in the serum of nanotube-treated mice 5 min, 3 days, and 14 days after injection (data not shown). Since PEG-SWCNTs are known to undergo renal excretion

(see ref 27) and our previous data showed that spleen and liver of mice systemically treated with PEG-SWCNT-750 exhibit a NIR signal detectable by the IVIS Spectrum system (see ref 23), we concluded that IA-PEG-SWCNT-750 were readily excreted *via* the renal route as soon as they exited the joints, leading to minimal, if any, accumulation in major organs. Taken together, our findings suggested that IA-injected PEG-SWCNTs persisted for a prolonged interval of time in both healthy and OA joints without accumulating into major organs or eliciting systemic side effects.

Internalization of IA-Injected PEG-SWCNTs into Chondrocytes. We next investigated the cartilage trafficking of PEG-SWCNTs, that is, if they were able to penetrate the cartilage extracellular matrix (ECM) and reach the chondrocytes. First, both the cultured human TC-28 chondrocyte cell line and purified primary bovine chondrocytes were incubated with 10 nM of PEG-SWCNT-650 (or equivalent volume of vehicle, PBS, as control) for 24 h. Fluorescence-activated cell sorting (FACS) analysis and confocal images provided evidence that PEG-SWCNT-650 were taken up by both chondrocyte cell lines with an efficiency very close to 100% and accumulated in the cytoplasm (Supporting Information, Figure S2A and B). Next, bovine cartilage explants were incubated with 10 nM of PEG-SWCNT-650 or equivalent volume of vehicle for 7 days, then fixed, embedded in Optimal Cutting Temperature (OCT) compound and sectioned by a microtome-cryostat. Confocal images of cartilage cryosections showed that PEG-SWCNT-650 could penetrate the cartilage ECM and the chondrocyte membrane to reach the cytoplasm and nucleus of chondrocytes (Supporting Information, Figure S2C). Finally, we investigated the trafficking of PEG-SWCNTs in healthy and OA cartilage ECMs and assessed whether these particles can penetrate chondrocytes *in vivo*. A set ($N = 9$) of healthy 4-month-old B6 mice was unilaterally IA-injected with 5 μg of PEG-SWCNT-650 in the knee. An additional set ($N = 9$) of 4-month-old B6 mice with OA (2 months post-DMM surgery) was unilaterally IA-injected with 5 μg of PEG-SWCNT-650 in the OA knee. Contralateral (healthy) knees were IA-injected with equal volume of vehicle (PBS, control). Each set was divided into 3 groups ($N = 3$) and sacrificed after 1, 3, and 14 days. The knees were collected, fixed, decalcified, embedded in OCT, and sliced. Histological slices were analyzed by confocal microscopy. In both healthy and OA mice, PEG-SWCNT-650 were almost exclusively found in the cell-free ECM immediately beneath the cartilage surface 1 day after IA administration, whereas, after 3 days, they were also found in the cytoplasm and nucleus of chondrocytes residing in the superficial cartilage. Intracellular particles were still evident 14 days after IA administration (Figure 3).

IA-Injected PEG-SWCNTs Do Not Worsen OA in DMM Mice. We have shown that IA-PEG-SWCNTs can enter chondrocytes in the superficial zone of the cartilage. The ability of our nanocarriers to penetrate superficial chondrocytes is relevant to the design of nanodrugs for OA, since superficial chondrocytes have been shown to contribute to cartilage catabolism in OA to a greater extent than chondrocytes in the deeper zone of cartilage.[5] However, it also raises the possibility that IA-PEG-SWCNTs might cause dysfunction of this important cell layer, thus worsening OA *per se*. In order to rule out this scenario, two groups ($N = 4$) of 2-month-old B6 mice received DMM surgery and were treated with either IA-PEG-SWCNTs or an equal volume of vehicle (control), respectively, in the OA knee. After 2 months, treated knees were collected, fixed, decalcified, and embedded in paraffin. Six micrometer thick frontal sections were taken, stained with Safranin-O, and counterstained with Fastgreen and Hematoxylin. Cartilage damage was examined on the four knee quadrants and scored using the Osteoarthritis Research Society International (OARSI) method.[28] We found no statistically significant worsening of pathology in knees from IA-PEG-SWCNT-treated OA mice relative to control knees (Figure 4A and B).

Possible proinflammatory effects of IA-PEG-SWCNTs *in vivo* were also investigated by measuring the expression level of interleukin-1 (IL-1) and tumor necrosis factor α (TNFα), two important pro-inflammatory cytokines which are expressed in OA joints and contribute to OA progression.[1] Immunohistochemistry (IHC) of cartilage slices showed that IA-injection of PEG-SWCNTs did not enhance expression of IL-1 or TNFα in OA knees (Figure 4C). We conclude that IA-PEG-SWCNTs are unlikely to worsen OA *per se*.

IA-Injected PEG-SWCNTs Deliver Anti-GFP Morpholino ASOs in Chondrocytes. In order to collect proof of principle evidence that IA-PEG-SWCNTs enable delivery of agents into chondrocytes *in vivo*, we developed PEG-SWCNT-650 carrying anti-GFP mASOs (PEG-SWCNT-mASOs) and assessed their ability to elicit GFP silencing in chondrocytes of healthy and OA GFP-transgenic mice. We chose mASOs as cargo, because they are validated tools to regulate gene expression in cells.[29] *In vitro* data showed that incubation of cells with free GFP-mASOs did not inhibit GFP expression (Supporting Information, Figure S3A). Additionally, IA-injected free GFP-mASOs displayed very short residence time in the joints (Supporting Information, Figure S4A) and poor penetration in the cartilage (Supporting Information, Figure S4B).

We found that mASOs efficiently adsorbed onto PEG-SWCNTs, likely *via* π-stacking of the nitrogenous bases onto exposed (non-PEGylated) portions of nanotube sidewalls. Thus, we assessed whether PEG-SWCNTs can deliver mASOs into chondrocytes and elicit gene inhibition *in vivo*. First, we assessed the ability of PEG-SWCNTs to deliver mASOs into cells *in vitro*. Since transfection of chondrocytes is technically challenging,

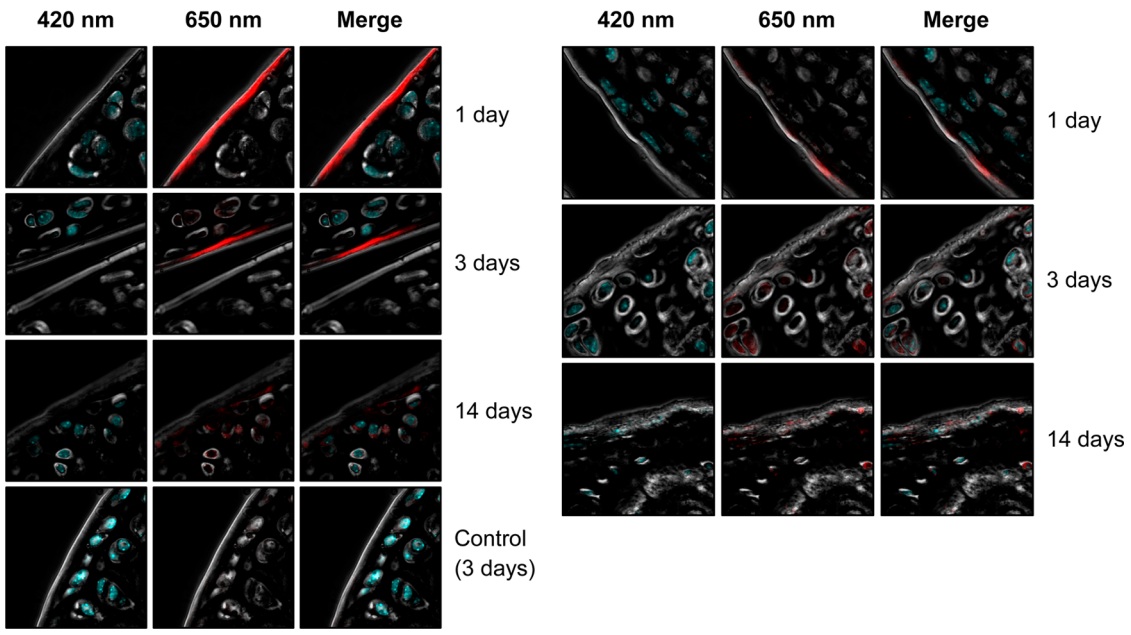

Figure 3. Cartilage ECM trafficking and chondrocyte internalization of IA-injected PEG-SWCNTs. (A) Five micrograms of PEG-SWCNT-650 in 10 μL of PBS was unilaterally IA-injected in the knees of healthy 4-month-old female B6 mice. Contralateral knees were IA-treated with equal volume of vehicle (PBS, control). (B) OA was induced in 2 month old female B6 mice by means of surgical destabilization of medial meniscus (DMM). After 2 months, 5 μg of PEG-SWCNT-650 in 10 μL of PBS was IA-injected in the OA knee. Contralateral (healthy) knees were IA-injected with equal volume of vehicle (PBS, control). Mice were divided in three groups (N = 3) and sacrificed 1, 3, or 14 days after IA administration. Knees were collected, fixed, decalcified, embedded in OCT, and sliced. Confocal images of cartilage cryosections showed that, in both healthy and OA mice, PEG-SWCNT-650 were almost exclusively found in the cell-free ECM immediately beneath the cartilage surface 1 day after IA administration, whereas they were also found in the cytoplasm and nucleus of chondrocytes residing in the superficial cartilage 3 days after administration. Particles were still found inside the chondrocytes 14 days after administration. No NIR fluorescence was detected from control knees.

we used lipofected human embryonic kidney (HEK) 293T cells to validate the ability of mASO-loaded PEG-SWCNTs to inhibit gene expression *in vitro*. Three hours after transfection of a GFP-encoding pEGFP-N1 plasmid, cells were incubated with 10 nM of PEG-SWCNT-mASOs for 48 h. Negative control cells were treated with 10 nM of PEG-SWCNTs loaded with nontargeting (control) mASOs (PEG-SWCNT-Ctr). Positive control cells were colipofected with pEGFP-N1 plasmid and an equivalent amount (~500 nM) of free GFP-mASOs. FACS analysis showed a significant decrease in the GFP signal in PEG-SWCNT-mASO-treated cells relatively to negative control-treated cells (Supporting Information, Figure S3A and B). Next, we investigated the ability of IA-injected PEG-SWCNTs to deliver mASOs into chondrocytes *in vivo*. A group (N = 3) of healthy 4-month-old GFP-transgenic [C57BL/6-Tg(UBC-GFP)30Scha/J] mice was unilaterally IA-treated with IA-PEG-SWCNT-mASOs in the knee. Contralateral knees were treated with PEG-SWCNT-Ctr. After 3 days, knees were collected and cryosections prepared. Confocal images of cryosections showed that, in IA-PEG-SWCNT-mASO-treated mice, nanotube-positive chondrocytes (cells in the yellow oval, Figure 5A) had faint GFP signal, whereas nanotube-negative cells (cells in the cyan oval, Figure 5A) exhibited bright GFP signal. Both nanotube-positive (upper panels, Figure S3C (Supporting Information)) and -negative (lower panels, Figure S3C (Supporting Information)) cells of IA-PEG-SWCNT-Ctr-treated (control) mice exhibited a strong GFP signal. We quantitated GFP (emission at 520 nm) and PEG-SWCNT (emission at 650 nm) signals by means of ImageJ and calculated the GFP/nanotube signal ratio to compare GFP signal in nanotube-positive chondrocytes of IA-PEG-SWCNT-mASO-treated and control mice. The average GFP/nanotube ratio was significantly lower in chondrocytes of IA-PEG-SWCNT-mASO-treated mice than in cells of control mice, suggesting that IA-PEG-SWCNTs can deliver mASOs and elicit gene silencing in chondrocytes of healthy mice (Figure 5B).

Finally, we investigated if PEG-SWCNTs were able to elicit GFP silencing in chondrocytes of GFP-transgenic mice with OA. A group of 4-month-old GFP-transgenic mice with OA was treated with IA-PEG-SWCNT-mASOs in the arthritic knee. After 3 days, treated knees were collected, cryosections prepared, and confocal images recorded. Similar to healthy animals, IA-PEG-SWCNT-mASO-positive chondrocytes (cell in the yellow oval, Figure 5C) had faint GFP signal, whereas nanotube-negative cells (cell in the cyan oval, Figure 5C)

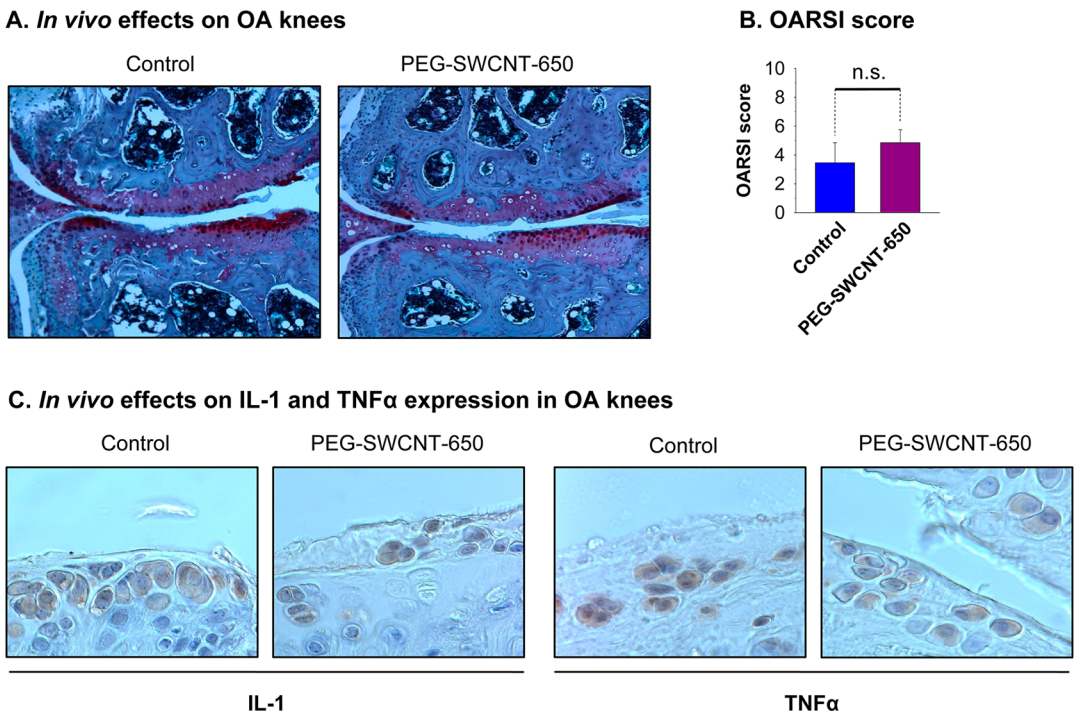

Figure 4. *In vivo* **effects of IA-injected PEG-SWCNTs. Two groups (*N* = 4) of 2-month-old female B6 mice received DMM surgery and were IA-injected with either 5 μg of IA-PEG-SWCNTs in 10 μL of PBS or an equal volume of vehicle (PBS, control), in the OA knee. After 2 months, OA knees were collected, fixed, decalcified, and embedded in paraffin. Six micrometer thick frontal sections were taken at 60 μm intervals and stained with Safranin-O and counterstained with Fastgreen and Hematoxylin (A). Cartilage damage was examined on the four knee quadrants and scored using the OARSI method. There was no statistically significant cartilage worsening in PEG-SWCNT-650-treated knees respect to control knees. Statistics: nonparametric Mann−Whitney U analysis (n.s. = not significant) (B). Alternatively, sections were stained with either anti-IL-1 or anti-TNFα antibodies. IL-1 and TNFα expression was examined on the four knee quadrants. There was no protein overexpression in PEG-SWCNT-650-treated knees respect to control knees of OA mice (C).**

exhibited bright GFP signal. Overall, our results validate our PEG-SWCNTs as efficient and safe systems to regulate the expression of specific genes in both homeostatic and hypertrophic chondrocytes *in vivo*.

DISCUSSION

Osteoarthritis (OA), often called wear-and-tear arthritis, is a degenerative disease of articular joints caused by an imbalance between anabolic (cartilage-producing) and catabolic (cartilage-degrading) states of cartilage-resident chondrocytes.[4] Over time, it leads to degradation of articular cartilage, variable joint inflammation and irreversible structural damage of the bone. OA symptoms can be controlled with systemic nonsteroidal anti-inflammatory drugs (NSAIDs) and IA hyaluronic acid (HA)-based viscosupplementation or glucocorticoids. However, no agent is currently available that can stop or slow down disease progression.[3] Modifying OA progression through pharmacologic manipulation of chondrocyte function is currently one of the largest unmet medical needs in rheumatology.

Although several studies have investigated the use of IA-injected liposomes and polymeric particles to improve the therapeutic index of antiarthritic drugs, their cartilage trafficking and efficacy to deliver cargo into chondrocytes of OA mice has not been assessed as of yet.[14] Penetration into chondrocytes essentially depends on the capability of IA-injected particles to persist in the synovial cavity for a prolonged time and enter the cartilage ECM. The latter is a 3D biomaterial composed by a covalently cross-linked collagen meshwork with a pore size of ~60 nm interpenetrated by negatively charged proteoglycans (i.e., chondroitin sulfate) and nonproteoglycan polysaccharides (i.e., HA).[15] SWCNTs modified with PEG chains using either covalently or noncovalently protocols have been extensively and successfully used to deliver drugs into cells residing in healthy and diseased tissues.[18] Due to their 1D structure, PEG-modified SWCNTs have been loaded with large and diversified drug payloads and efficiently entered tumor tissues.[19,30−34] We recently investigated the pattern of plasma proteins (the "blood" protein corona) adsorbed onto PEG-modified SWCNTs and found that the relative abundance of HA-binding proteins such as α-1 microglobulin was significantly higher in the protein corona of SWCNTs noncovalently modified with PEG chains (PEG-coated SWCNTs or PEG-SWCNTs) than in plasma.[23] Due to the unique physicochemical properties (1D structure and diameter smaller than 10 nm) of PEG-SWCNTs and the possible presence of certain HA-binding proteins on their surface, we wondered whether these particles could enter

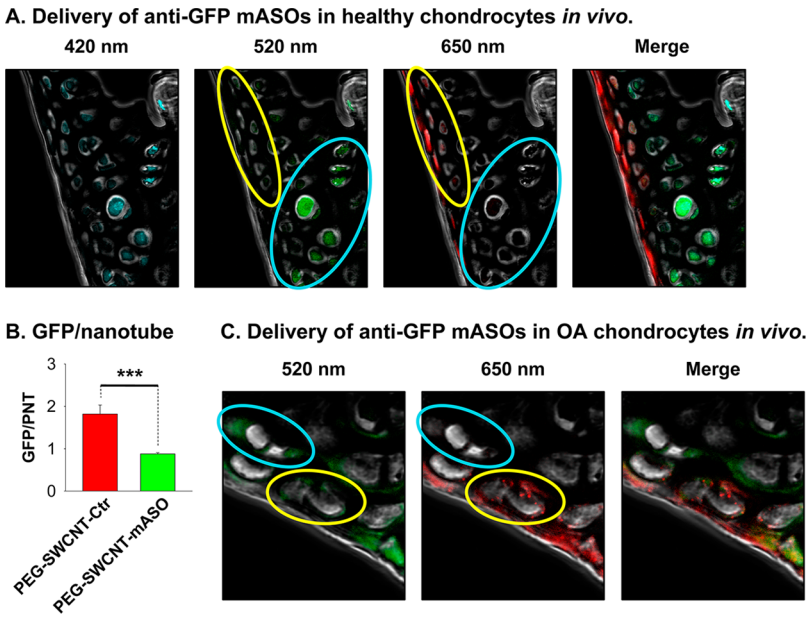

Figure 5. (A, B) Delivery of anti-GFP mASOs by IA-injected PEG-SWCNTs in healthy chondrocytes *in vivo*. Healthy ($N = 3$) female C57BL/6-Tg(UBC-GFP)30Scha/J mice were unilaterally IA-treated in the knee with 5 μg of PEG-SWCNT-mASOs in 10 μL of PBS. Contralateral knees were treated with PEG-SWCNT-Ctr. After 3 days, mice were sacrificed and cartilage cryosections prepared. Confocal images showed that nanotube-positive chondrocytes (650 nm signal) of IA-PEG-SWCNT-mASO-treated mice had faint GFP fluorescence (*i.e.*, cells inside yellow oval), whereas nanotube-negative cells (*i.e.*, cells inside cyan oval) had bright GFP signal. In contrast, both nanotube-positive and -negative cells of IA-PEG-SWCNT-Ctr-treated mice had bright GFP signal (see Figure S6C, Supporting Information). (B) GFP and PEG-SWCNT-650 signals were quantitated for nanotube-positive cells in four microscopic fields recorded for each of the six cartilage sections collected for IA-PEG-SWCNT-mASO- and IA-PEG-SWCNT-Ctr-treated knees, and the GFP/nanotube signal ratio calculated. Statistics: nonparametric Mann−Whitney U analysis (*$p < 0.001$). (C) Delivery of anti-GFP mASOs by IA-injected PEG-SWCNTs in OA chondrocytes *in vivo*. Four-month-old female C57BL/6-Tg(UBC-GFP)30Scha/J mice with OA (2 months post-DMM surgery) were injected in the OA knee with 5 μg of PEG-SWCNT-mASOs in 10 μL of PBS. After 3 days mice, were sacrificed and cartilage cryosections prepared. Confocal images showed that nanotube-positive chondrocytes (650 nm signal) had faint GFP fluorescence (*i.e.*, cells inside yellow oval), whereas nanotube-negative cells (*i.e.*, cells inside cyan oval) had bright GFP signal.**

and navigate into the cartilage meshwork and deliver cargo into chondrocytes. Here we show that IA-injected PEG-SWCNTs persisted for long time into the synovial cavity, entered the cartilage ECM, delivered morpholino antisense oligonucleotides (mASOs) into chondrocytes and regulated the expression of the mASO-targeted gene in chondrocytes of both healthy and OA mice. Moreover, we show that IA-PEG-SWCNTs did not elicit systemic or regional side effects. Thus, we propose that PEG-SWCNTs can be used as safe scaffolds for the fabrication of therapeutic systems capable to deliver DMOADs into chondrocytes and reestablish cartilage homeostasis.

In this study, SWCNTs were first modified (coated) with 2 kDa MW PEG chains (PEG-SWCNTs) through the adsorption of PEG-modified phospholipids and next loaded with mASOs (PEG-SWCNT-mASOs).[21] Approximately 50 mASO molecules adsorbed onto each particle. AFM imaging showed that our particles were individually dispersed and had an average length of ~110 nm. We also used AFM imaging to investigate the conformation of PEG chains onto PEG-SWCNTs and PEG-SWCNT-mASOs. In line with previous reports about the behavior of PEG-modified phospholipids on hydrophobic surfaces, we found that PEG-modified phospholipids did not uniformly coat the nanotubes' sidewalls and exposed (uncoated) portions of the graphitic surface were found in ~50% of PEG-SWCNTs.[35] This result was also consistent with other reports that exposed portions of nanotubes' sidewalls enable the adsorption of polyaromatic small molecules (*i.e.*, paclitaxel, doxorubicin) onto PEG-SWCNTs *via* π-stacking and their transport into cancer cells.[31,32] Thus, we reasoned that mASOs could be loaded onto PEG-SWCNTs *via* π-stacking of nitrogenous bases onto the exposed portions of nanotubes' sidewalls. AFM imaging confirmed loading of mASOs onto PEG-SWCNTs by showing that PEG-SWCNT-mASOs lacked exposed portions of the graphitic sidewalls and that the average height of the polymer shell of PEG-SWCNT-mASOs was more than 2-fold higher than that of PEG-SWCNTs (~3.1 nm vs ~1.4 nm) (Figure 1).

When assessing the joint persistence time of IA-PEG-SWCNTs, we found that while IA-injected free fluorochromes exited the joints in less than 8 h, more than 25% of the starting dose of IA-PEG-SWCNTs was retained in healthy joints 14 days after administration. Additionally, we found that the particles' elimination rate from the joints was not significantly increased in OA mice. Although OA joints are characterized by leaky blood vessels (ref 25), which might enhance particle clearance from the joint space, we hypothesized that

dynamic compression during ambulation may push PEG-SWCNTs against the cartilage surface as soon as they enter the synovial fluid (SF), thus favoring their quick penetration into the cartilage. Also, the possible presence of HA-binding α-1 microglobulin on the protein corona adsorbed onto IA-PEG-SWCNTs in the SF (the "synovial" protein corona) might favor interaction of the particles with HA in the SF, thus increasing joint retention.[23]

Next, we showed that IA-PEG-SWCNTs have the ability to enter the cartilage ECM and accumulate into chondrocytes *in vivo* in both healthy and OA mice. PEG-SWCNTs broke through the ECM barrier and accumulated inside the cytoplasm and nucleus of chondrocytes as early as 3 days after IA-injection in healthy and OA joints. To the best of our knowledge, this was the first report about the trafficking of nonviral delivery systems in OA cartilage.

Only two reports described the trafficking of nonviral IA-injected spherical nanoparticles in healthy cartilage.[16,17] These studies showed that certain properties of the "synthetic" identity (*i.e.*, size, surface charge and surface conjugation) influence the particles' cartilage trafficking, that is, only positively charged spherical particles with a diameter smaller than the cartilage meshwork size (~60 nm) entered the ECM and surface conjugation with targeting moieties made it possible to accumulate the nanoparticles in specific cartilage sites (i.e., chondrocytes or ECM). Surprisingly, PEG-SWCNTs display good cartilage penetration despite their surface charge of approximately −11 mV (in PBS). It is possible that a synovial corona enriched in HA-binding proteins along with their 1D structure, diameter smaller than 10 nm, and convective transport of fluid between the synovial cavity and ECM during ambulation overcame the repelling effect of surface charge, ultimately favoring the navigation of PEG-SWCNTs through the ECM. In the future, conjugation of PEG-SWCNTs to targeting agents against chondrocytes might enable tuning of cartilage trafficking of PEG-SWCNTs.

It is worth noting that, whereas spherical nanoparticles described in ref 16 accumulated into the cytoplasm of chondrocytes and did not enter the nucleus, PEG-SWCNTs were found in both the cytoplasm and nucleus of chondrocytes following IA injection in healthy and OA joints. Although the mechanisms of chondrocyte internalization and nuclear translocation of PEG-SWCNTs remain to be clarified, our results are consistent with previous reports showing that only individual short nanotubes can enter the cell nucleus.[36] Our nanotubes were individual and had an average length of ~110 nm, and thus had the required properties for nuclear accumulation.

IA-PEG-SWCNTs did not accumulate into major organs and did not alter liver function in both healthy and OA mice. Additionally the particles did not worsen OA in mice. Our data suggest that the pharmacokinetic profile of IA-PEG-SWCNTs is different from SA-PEG-SWCNTs, which accumulated into Kupffer cells.[18,22] This difference may be explained by the fact that SA-PEG-SWCNTs are likely aggregate as soon as they enter the bloodstream due to high local blood concentration, thus triggering uptake by macrophages and accumulation into the organs of the reticuloendothelial system (RES). In contrast, IA-PEG-SWCNTs are slowly released from the joints; thus, they likely remain individually dispersed in the bloodstream, avoiding uptake by RES macrophages and efficiently reaching the glomerular filtration system.[27] In addition, since we have recently reported that the protein corona affect the PEG-SWCNTs' biological performance, differences between the "blood" protein corona of SA-PEG-SWCNTs and the "synovial" protein corona of IA-PEG-SWCNTs might also explain their different pharmacokinetics.[23] Since not all the proteins of the synovial protein corona are exchanged with blood proteins after IA-PEG-SWCNTs enter the bloodstream, the final protein corona on IA-PEG-SWCNTs is likely to be a mixture of proteins from the synovial fluid and the blood, a "synovial-blood" protein corona.[37]

Finally, to the best of our knowledge, the present study is the first report about the delivery of mASOs in articular cartilage *in vivo*. mASOs are considered the knockdown reagent of choice for *in vivo* experiments because of their excellent stability against nuclease digestion, high target specificity, and poor immunogenicity.[29] Nevertheless, free mASOs tend to remain trapped in the endolysosomal compartments, which is a critical barrier to their intracellular delivery and suggests that coupling with appropriate DDSs might be useful to exploit mASOs as cell-specific gene inhibitors.[29] Our data points to the usefulness of PEG-SWCNTs as DDSs of choice for chondrocyte delivery of mASOs, paving the way to their use for validation of new genetic targets to reestablish chondrocyte homeostasis in OA.

CONCLUSION

The use of locally administered DDSs to accumulate DMOADs into chondrocytes and manipulate cell function has been envisaged as the next frontier in the treatment of OA. The choice of a particle to deliver cargo into a specific tissue needs to take into account the physiology peculiar to the tissue and both the "synthetic" and "biological" identities of the particle. These properties are intimately related. It has been described that particle "biological" identity, that is, the "corona" of biomolecules adsorbed onto particles as soon as they come into contact with the biological milieu, mediates the influence of particle physical and chemical properties—the "synthetic" identity—on downstream biological outcomes.[23,38−41] In the context of the development of chondrocyte-specific DDSs,

the particle "synthetic" identity and SF composition will determine the corona adsorbed onto IA-injected particles, which, in turn, will affect their ability to navigate through the cartilage ECM and enter chondrocytes and, ultimately, their therapeutic index (i.e., collagen production and chondrocyte homeostasis) and pharmacokinetic profile (i.e., accumulation into major organs and clearance).

Herein, we describe an efficient nonviral IA DDS based on PEG-SWCNTs. After a single IA injection, PEG-SWCNTs were able to efficiently enter the dense cartilage ECM, translocate into the cytoplasm of chondrocytes, and deliver gene inhibitors without affecting cartilage homeostasis or elicit systemic side-effects. The strategy followed in this study to investigate downstream biological outcomes of PEG-SWCNTs fabricated by noncovalently modifying SWCNTs with 2 kDa MW linear PEG chains can be easily extended to SWCNTs covalently or noncovalently modified with PEG chains of different nature (linear vs branched), length, and/or morphology (mushroom vs brush conformation). Further studies focused on the "synovial" corona and biodegradation of IA-injected PEG-SWCNTs are warranted to unravel the molecular mechanisms driving their downstream biological outcomes and translate these particles into clinical trials.[42,43]

MATERIALS AND METHODS

Fabrication and Characterization of PEG-Modified SWCNTs. Amino-functionalized PEG-SWCNTs were fabricated through the adsorption of phospholipids modified with amino-terminated 2 kDa molecular weight (MW) linear PEG chains (DSPE-PEG2000) (Avanti Polar Lipids, Inc., Alabaster, AL) by following our published protocol. First, 5 mg of pristine (nonfunctionalized) SWCNTs (Carbon Solutions, Inc., Riverside, CA) was dried at 160 °C for 3 h and sonicated with DSPE-PEG2000 in PBS by using an ultrasonic bath for 6 h. Next, the mixture was fractionated by stepwise centrifugation to isolate short (amino-terminated) PEG-SWCNTs and washed eight times through 100 kDa MW cutoff filtration devices in Milli-Q H_2O to remove free phospholipids. PEG-SWCNTs carrying 650 or 750 nm emitting fluorochromes (PEG-SWCNT-650 or PEG-SWCNT-750, respectively) were fabricated by incubating amino-terminated PEG-SWCNTs with fluorochromes carrying activated carboxyl groups (NHS-Seta650 or NHS-Seta750, SETA BioMedicals, Urbana, IL) for 24 h at room temperature and purified by filtration.

The value of PEG density was obtained by calculating the concentration of both amino groups on amino-terminated PEG-SWCNTs by Kaiser Test and fluorochromes on PEG-SWCNT-750 by absorbance spectroscopy.

PEG-SWCNTs loaded with GFP-mASOs (targeting mASO; sequence: 5′-acagctcctcgcccttgctcaccat-3′) (PEG-SWCNT-mASOs) or control mASOs (nontargeting mASO; sequence: 5′-ggtggattgccttttcagctt-3′) (PEG-SWCNT-Ctr) were fabricated by incubating PEG-SWCNT-650 with mASOs in PBS o/n at 4 °C and subsequent washing through 100 kDa MW cutoff filtration devices in PBS to remove free oligos. Eluate solutions from filtration were collected, and the absorbance spectra recorded. The absorbance value at 260 nm was used to calculate mASO concentration in eluate solutions and, in turn, the number of mASO molecules adsorbed onto the nanotubes. The number of mASO molecules per PEG-SWCNT was calculated by considering the PEG-SWCNTs' MW equal to approximately 250 kDa (see ref 20).

The stability of mASOs adsorbed onto PEG-SWCNTs was tested by keeping PEG-SWCNT-mASOs at room temperature for several hours and washing them once through 100 kDa MW cutoff filtration devices in PBS. Eluate solution from filtration was collected and the absorbance spectrum recorded to assess the release of molecules from PEG-SWCNTs.

AFM Imaging. Five microliters of amino-terminated PEG-SWCNTs (or PEG-SWCNT-mASOs) in PBS was dropped onto a freshly cleaved mica substrate (Ted Pella, Inc., Redding, CA) and allowed to stand for 5 min. The mica surface was rinsed with Milli-Q H_2O and dried under N_2 stream. AFM images were recorded through an 5500 atomic force microscope (Agilent Technologies, Inc., Santa Clara, CA) in noncontact (AAC) mode.

Cartilage ECM Trafficking and Chondrocyte Internalization *in Vitro*. Human TC-28 cells, bovine chondrocytes, and bovine cartilage blocks were provided from Dr. Liu Bryan's lab. All the samples were cultured in DMEM (Mediatech, Inc., Manassas, VA) with 10% FBS (Omega Scientific, Inc., Tarzana, CA) with 5% CO_2 at 37 °C and incubated with 10 nM of PEG-SWCNT-650 or equal volume of vehicle (PBS, control) for 24 h. Then, cells were analyzed *via* FACS (LSR-II Flow Cytometer, Becton Dickinson and Company, Franklin Lakes, NJ) and confocal microscopy (FluoView FV10i, Olympus, Center Valley, PA). Cartilage blocks were fixed in 10% neutral buffered zinc-formalin (Thermo Fisher Scientific, Logan, UT) for 48 h and frozen in optimum cutting compound (OCT). Six micrometer thick slides were obtained by means of a cryostat and analyzed through confocal microscopy.

Destabilization of Medial Meniscus. All animal experiments were carried out in accordance with Institutional Animal Care and Use Committee-approved protocols at the La Jolla Institute for Allergy & Immunology (La Jolla, CA). All efforts were made to minimize animal suffering. Destabilization of medial meniscus (DMM) was induced in the left knees of 2-month-old female C57BL/6J and C57BL/6-Tg(UBC-GFP)30Scha/J mice (The Jackson Laboratory, Bar Harbor, ME) by transection of the anteromedial meniscotibial and medial collateral ligaments.

Joint Persistence and Organ Accumulation. Five micrograms of PEG-SWCNT-750 in 10 μL of PBS was unilaterally IA-injected into the knees of a group (N = 5) of healthy 3-month-old female C57BL/6J mice and in the arthritic knees of a group (N = 5) of 3-month-old female C57BL/6J mice with OA (1 month post-DMM surgery). Joint residence time of PEG-SWCNT-750 was followed by recording the NIR emission from treated joints by means of an IVIS Spectrum Pre-Clinical *In Vivo* Imaging System (PerkinElmer, Waltham, MA) at days 0, 1, 3, 7, and 14. Then the mice were sacrificed, the organs extracted and tested for the presence of PEG-SWCNT-750, and the blood used to test alanine transaminase (ALT), aspartate transaminase (AST), and creatinine levels by using commercial kits (BioAssay Systems, Hayward, CA). A control group (N = 5) of healthy 3-month-old female C57BL/6J mice was unilaterally IA-injected in the knee with an equivalent amount of free 750 nm emitting fluorochromes (Seta750, SETA BioMedicals), and the NIR emission of treated knees was followed for 8 h. An additional control group (N = 3) of healthy 3-month-old female C57BL/6J mice was unilaterally IA-injected in the knee with 1 nmol of fluorescein-labeled control mASO in 10 μL of PBS. Contralateral knees were injected with 10 μL of PBS. Animal NIR images were recorded after 5 min, 24 h, 48 h, and 72 h.

Cartilage ECM Trafficking and Chondrocyte Internalization *in Vivo*. A set (N = 9) of 4-month-old female C57BL/6J mice were unilaterally IA-injected in the knee with 5 μg of PEG-SWCNT-650 in 10 μL of PBS. The set was divided into three groups (N = 3), and each group was sacrificed 1, 3, or 14 days after administration. An additional set (N = 9) of 2-month-old female C57BL/6J mice received DMM surgery, were IA treated with 5 μg of PEG-SWCNT-650 in the OA knee 2 months after surgery, and divided in three groups. Each group was sacrificed 1, 3, or 14 days after administration. Knees were harvested, fixed in 10% neutral buffered zinc-formalin (Thermo Fisher Scientific) for 48 h,

decalcified in Cal-Ex II solution (Thermo Fisher Scientific) for 4 days, and frozen in OCT. Six micrometer thick slides were obtained with a cryostat from each knee, stained with Hoechst, and analyzed by means of confocal microscopy.

A control group (N = 3) of healthy 3-month-old female C57BL/6J mice was unilaterally IA-injected in the knee with 1 nmol of fluorescein-labeled control mASO in 10 μL of PBS. Contralateral knees were injected with 10 μL of PBS. After 3 days, mice were sacrificed and the cryosections prepared and analyzed by means of a confocal microscope.

***In Vivo* Effects.** DMM was induced in two groups (N = 4) of 2-month-old female C57BL/6J mice. Two months after surgery, one group of mice was IA-injected in the OA knee with 5 μg of PEG-SWCNT-650 in 10 μL of PBS, whereas the other group was treated with an equal volume of vehicle (PBS, control). Both groups of mice were sacrificed at the age of 6 months. Knees were harvested, fixed in 10% neutral buffered zinc-formalin for 48 h, decalcified in Cal-Ex II solution for 4 days, and embedded in paraffin using standard protocols. Six micrometer thick frontal coronal sections were cut at an interval of ~60 μm. Fifteen slides were stained with Safranin-O Fast-Green technique and analyzed with the OARSI scoring system. Extra slides from each knee were processed for IL-1 and TNFα immunohistochemistry. Briefly, slides were pretreated with boiling citrate buffer antigen retrieval (1.9 mM citric acid, 10 mM tris-sodium citrate pH 6.0) for 10 min and then were treated with 3% H_2O_2 for 10 min. Slides were then blocked with 5% bovine serum albumin at 4 °C o/n. Antibodies anti-IL-1 (Abcam, Cambridge, UK) and anti-TNFα (Santa Cruz Biotechnology, Inc., Dallas, TX) (1:200 in 5% bovine serum albumin) were incubated with the samples at 4 °C o/n. Next, the slides were incubated with secondary peroxidase-conjugated antibodies (Vector Laboratories, Inc., Burlingame, CA) for 30 min at room temperature. Signal detection was obtained incubating the samples for 5 min with 3,3′-diaminobenzidine substrate (Sigma-Aldrich, St. Louis, MO). Images were collected with an Eclipse 80i microscope (Nikon, Inc., Melville, NY).

***In Vitro* Silencing of Gene Expression.** Hek293T cells were lipofected (Lipofectamine 2000, Sigma-Aldrich, St. Louis, MO) with pEGFP-N1 plasmid (kindly gifted by Prof. Amnon Altman's laboratory, La Jolla Institute for Allergy and Immunology, La Jolla, CA) and incubated with 1 nM of PEG-SWCNT-mASOs, 1 nM of PEG-SWCNT-Ctr, an an equivalent amount of free GFP-mASOs or colipofected with an equivalent amount of free GFP-mASOs. Cells were analyzed by FACS after 48 h.

***In Vivo* Silencing of Gene Expression.** One group (N = 3) of healthy 4-month-old female C57BL/6-Tg(UBC-GFP)30Scha/J mice was unilaterally IA-treated in the knee with 5 μg of IA-PEG-SWCNT-mASOs in 10 μL of PBS. Contralateral knees were treated with IA-PEG-SWCNT-Ctr. An additional group (N = 2) of 4-month-old female C57BL/6-Tg(UBC-GFP)30Scha/J mice with OA (2 months post-DMM surgery) was treated in the arthritic knee with 5 μg of IA-PEG-SWCNT-mASOs in 10 μL of PBS. Mice were sacrificed after 3 days, and knees were harvested, fixed in 10% neutral buffered zinc-formalin for 48 h, decalcified in Cal-Ex II solution for 4 days, and frozen in OCT. Ten 6 μm thick slides were cut by means of a cryostat for each knee and stained with Hoechst. GFP/nanotube signal ratio was obtained through a FluoView FV10i confocal microscope.

Statistical Analysis. Nonparametric Mann−Whitney U analysis was performed by using SPSS Statistics software (IBM Corporation, Armonk, NY).

Conflict of Interest: The authors declare no competing financial interest.

Supporting Information Available: Joint persistence of IA-injected free fluorochromes; Effects of IA-injected PEG-SWCNTs on liver functions; Internalization of PEG-SWCNTs into cultured human TC-28 cells, extracted bovine chondrocytes and bovine cartilage explants; Delivery of anti-GFP mASOs by PEG-SWCNTs *in vitro*; Delivery of control mASOs by IA-injected PEG-SWCNTs in healthy chondrocytes *in vivo*; Joint persistence and cartilage trafficking of free control mASOs. This material is available free of charge *via* Internet at http://pubs.acs.org.

Acknowledgment. This work was supported by a grant from the Arthritis National Research Foundation (The John Vaughan Scholarship) to M.B and by LJI Institutional funds (to N.B.). We thank Dr. Jon D. Moulton (Gene Tools, LLC) for helpful comments. This is manuscript #1746 from LJI.

REFERENCES AND NOTES

1. Haseeb, A.; Haqqi, T. M. Immunopathogenesis of Osteoarthritis. *Clin. Immunol.* **2013**, *146*, 185–196.
2. Cross, M.; Smith, E.; Hoy, D.; Nolte, S.; Ackerman, I.; Fransen, M.; Bridgett, L.; Williams, S.; Guillemin, F.; Hill, C. L.; *et al.* The Global Burden of Hip and Knee Osteoarthritis: Estimates from the Global Burden of Disease 2010 Study. *Ann. Rheum. Dis.* **2014**, *73*, 1323–1330.
3. Jevsevar, D. S. Treatment of Osteoarthritis of the Knee: Evidence-Based Guideline, 2nd Edition. *J. Am. Acad. Orthop. Surg.* **2013**, *21*, 571−576.
4. van der Kraan, P. M.; van den Berg, W. B. Chondrocyte Hypertrophy and Osteoarthritis: Role in Initiation and Progression of Cartilage Degeneration? *Osteoarthritis Cartilage* **2012**, *20*, 223–232.
5. Aigner, T.; Vornehm, S. I.; Zeiler, G.; Dudhia, J.; von der Mark, K.; Bayliss, M. T. Suppression of Cartilage Matrix Gene Expression in Upper Zone Chondrocytes of Osteoarthritic Cartilage. *Arthritis Rheum.* **1997**, *40*, 562–569.
6. Husa, M.; Liu-Bryan, R.; Terkeltaub, R. Shifting HIFs in Osteoarthritis. *Nat. Med.* **2010**, *16*, 641–644.
7. Saito, T.; Fukai, A.; Mabuchi, A.; Ikeda, T.; Yano, F.; Ohba, S.; Nishida, N.; Akune, T.; Yoshimura, N.; Nakagawa, T.; *et al.* Transcriptional Regulation of Endochondral Ossification by HIF-2alpha during Skeletal Growth and Osteoarthritis Development. *Nat. Med.* **2010**, *16*, 678–686.
8. Yang, S.; Kim, J.; Ryu, J. H.; Oh, H.; Chun, C. H.; Kim, B. J.; Min, B. H.; Chun, J. S. Hypoxia-Inducible Factor-2alpha Is a Catabolic Regulator of Osteoarthritic Cartilage Destruction. *Nat. Med.* **2010**, *16*, 687–693.
9. Gerwin, N.; Hops, C.; Lucke, A. Intraarticular Drug Delivery in Osteoarthritis. *Adv. Drug Delivery Rev.* **2006**, *58*, 226–242.
10. Owen, S. G.; Francis, H. W.; Roberts, M. S. Disappearance Kinetics of Solutes from Synovial Fluid after Intra-Articular Injection. *Br. J. Clin. Pharmacol.* **1994**, *38*, 349–355.
11. Simkin, P. A. Synovial Perfusion and Synovial Fluid Solutes. *Ann. Rheum. Dis.* **1995**, *54*, 424–428.
12. Foy, B. D.; Blake, J. Diffusion of Paramagnetically Labeled Proteins in Cartilage: Enhancement of the 1-D NMR Imaging Technique. *J. Magn. Reson.* **2001**, *148*, 126–134.
13. Edwards, S. H. Intra-Articular Drug Delivery: the Challenge to Extend Drug Residence Time within the Joint. *Vet. J.* **2011**, *190*, 15–21.
14. Larsen, C.; Ostergaard, J.; Larsen, S. W.; Jensen, H.; Jacobsen, S.; Lindegaard, C.; Andersen, P. H. Intra-Articular Depot Formulation Principles: Role in the Management of Post-operative Pain and Arthritic Disorders. *J. Pharm. Sci.* **2008**, *97*, 4622–4654.
15. Martel-Pelletier, J.; Boileau, C.; Pelletier, J. P.; Roughley, P. J. Cartilage in Normal and Osteoarthritis Conditions. *Best Pract. Res., Clin. Rheumatol.* **2008**, *22*, 351–384.
16. Rothenfluh, D. A.; Bermudez, H.; O'Neil, C. P.; Hubbell, J. A. Biofunctional Polymer Nanoparticles for Intra-Articular Targeting and Retention in Cartilage. *Nat. Mater.* **2008**, *7*, 248–254.
17. Pi, Y.; Zhang, X.; Shi, J.; Zhu, J.; Chen, W.; Zhang, C.; Gao, W.; Zhou, C.; Ao, Y. Targeted Delivery of Non-Viral Vectors to Cartilage *in Vivo* Using a Chondrocyte-Homing Peptide Identified by Phage Display. *Biomaterials* **2011**, *32*, 6324–6332.
18. Bottini, M.; Rosato, N.; Bottini, N. PEG-Modified Carbon Nanotubes in Biomedicine: Current Status and Challenges Ahead. *Biomacromolecules* **2011**, *12*, 3381–3393.
19. Sacchetti, C.; Rapini, N.; Magrini, A.; Cirelli, E.; Bellucci, S.; Mattei, M.; Rosato, N.; Bottini, N.; Bottini, M. *In Vivo* Targeting of Intratumor Regulatory T Cells Using PEG-Modified Single-Walled Carbon Nanotubes. *Bioconjugate Chem.* **2013**, *24*, 852–858.

20. Delogu, L. G.; Magrini, A.; Bergamaschi, A.; Rosato, N.; Dawson, M. I.; Bottini, N.; Bottini, M. Conjugation of Antisense Oligonucleotides to PEGylated Carbon Nanotubes Enables Efficient Knockdown of PTPN22 in T Lymphocytes. *Bioconjugate Chem.* **2009**, *20*, 427–431.
21. Cato, M. H.; D'Annibale, F.; Mills, D. M.; Cerignoli, F.; Dawson, M. I.; Bergamaschi, E.; Bottini, N.; Magrini, A.; Bergamaschi, A.; Rosato, N.; *et al.* Cell-Type Specific and Cytoplasmic Targeting of PEGylated Carbon Nanotube-Based Nanoassemblies. *J. Nanosci. Nanotechnol.* **2008**, *8*, 2259–2269.
22. Schipper, M. L.; Nakayama-Ratchford, N.; Davis, C. R.; Kam, N. W.; Chu, P.; Liu, Z.; Sun, X.; Dai, H.; Gambhir, S. S. A Pilot Toxicology Study of Single-Walled Carbon Nanotubes in a Small Sample of Mice. *Nat. Nanotechnol.* **2008**, *3*, 216–221.
23. Sacchetti, C.; Motamedchaboki, K.; Magrini, A.; Palmieri, G.; Mattei, M.; Bernardini, S.; Rosato, N.; Bottini, N.; Bottini, M. Surface Polyethylene Glycol Conformation Influences the Protein Corona of Polyethylene Glycol-Modified Single-Walled Carbon Nanotubes: Potential Implications on Biological Performance. *ACS Nano* **2013**, *7*, 1974–1989.
24. Delogu, L. G.; Stanford, S. M.; Santelli, E.; Magrini, A.; Bergamaschi, A.; Motamedchaboki, K.; Rosato, N.; Mustelin, T.; Bottini, N.; Bottini, M. Carbon Nanotube-Based Nanocarriers: the Importance of Keeping it Clean. *J. Nanosci. Nanotechnol.* **2010**, *10*, 5293–5301.
25. Scanzello, C. R.; Goldring, S. R. The Role of Synovitis in Osteoarthritis Pathogenesis. *Bone* **2012**, *51*, 249–257.
26. Glasson, S. S.; Blanchet, T. J.; Morris, E. A. The Surgical Destabilization of the Medial Meniscus (DMM) Model of Osteoarthritis in the 129/SvEv Mouse. *Osteoarthritis Cartilage* **2007**, *15*, 1061–1069.
27. Al-Jamal, K. T.; Nunes, A.; Methven, L.; Ali-Boucetta, H.; Li, S.; Toma, F. M.; Herrero, M. A.; Al-Jamal, W. T.; ten Eikelder, H. M.; Foster, J.; *et al.* Degree of Chemical Functionalization of Carbon Nanotubes Determines Tissue Distribution and Excretion Profile. *Angew. Chem., Int. Ed. Engl.* **2012**, *51*, 6389–6393.
28. Glasson, S. S.; Chambers, M. G.; Van Den Berg, W. B.; Little, C. B. The OARSI Histopathology Initiative - Recommendations for Histological Assessments of Osteoarthritis in the Mouse. *Osteoarthritis Cartilage* **2010**, *18* (Suppl 3), S17–S23.
29. Summerton, J.; Weller, D. Morpholino Antisense Oligomers: Design, Preparation, and Properties. *Antisense Nucleic Acid Drug Dev.* **1997**, *7*, 187–195.
30. Liu, Z.; Cai, W.; He, L.; Nakayama, N.; Chen, K.; Sun, X.; Chen, X.; Dai, H. *In Vivo* Biodistribution and Highly Efficient Tumour Targeting of Carbon Nanotubes in Mice. *Nat. Nanotechnol.* **2007**, *2*, 47–52.
31. Liu, Z.; Sun, X.; Nakayama-Ratchford, N.; Dai, H. Supramolecular Chemistry on Water-Soluble Carbon Nanotubes for Drug Loading and Delivery. *ACS Nano* **2007**, *1*, 50–56.
32. Liu, Z.; Fan, A. C.; Rakhra, K.; Sherlock, S.; Goodwin, A.; Chen, X.; Yang, Q.; Felsher, D. W.; Dai, H. Supramolecular Stacking of Doxorubicin on Carbon Nanotubes for *in Vivo* Cancer Therapy. *Angew. Chem., Int. Ed. Engl.* **2009**, *48*, 7668–7672.
33. Lay, C. L.; Liu, H. Q.; Tan, H. R.; Liu, Y. Delivery of Paclitaxel by Physically Loading onto Poly-(Ethylene Glycol) (PEG)-Graft-Carbon Nanotubes for Potent Cancer Therapeutics. *Nanotechnology* **2010**, *21*, 065101.
34. Bottini, M.; Cerignoli, F.; Dawson, M. I.; Magrini, A.; Rosato, N.; Mustelin, T. Full-Length Single-Walled Carbon Nanotubes Decorated with Streptavidin-Conjugated Quantum Dots as Multivalent Intracellular Fluorescent Nanoprobes. *Biomacromolecules* **2006**, *7*, 2259–2263.
35. Du, H.; Chandaroy, P.; Hui, S. W. Grafted Poly-(Ethylene Glycol) on Lipid Surfaces Inhibits Protein Adsorption and Cell Adhesion. *Biochim. Biophys. Acta* **1997**, *1326*, 236–248.
36. Mu, Q.; Broughton, D. L.; Yan, B. Endosomal Leakage and Nuclear Translocation of Multiwalled Carbon Nanotubes: Developing a Model for Cell Uptake. *Nano Lett.* **2009**, *9*, 4370–4375.
37. Pietroiusti, A.; Campagnolo, L.; Fadeel, B. Interactions of Engineered Nanoparticles with Organs Protected by Internal Biological Barriers. *Small* **2013**, *9*, 1557–1572.
38. Monopoli, M. P.; Åberg, C.; Salvati, A.; Dawson, K. A. Biomolecular Coronas Provide the Biological Identity of Nanosized Materials. *Nat. Nanotechnol.* **2012**, *7*, 779–786.
39. Wang, F.; Yu, L.; Monopoli, M. P.; Sandin, P.; Mahon, E.; Salvati, A.; Dawson, K. A. The Biomolecular Corona is Retained During Nanoparticle Uptake and Protects the Cells from the Damage Induced by Cationic Nanoparticles until Degraded in the Lysosomes. *Nanomedicine* **2013**, *9*, 1159–1168.
40. Lesniak, A.; Fenaroli, F.; Monopoli, M. P.; Åberg, C.; Dawson, K. A.; Salvati, A. Effects of the Presence or Absence of a Protein Corona on Silica Nanoparticle Uptake and Impact on Cells. *ACS Nano* **2012**, *6*, 5845–5857.
41. Hu, G.; Jiao, B.; Shi, X.; Valle, R. P.; Fan, Q.; Zuo, Y. Y. Physicochemical Properties of Nanoparticles Regulate Translocation across Pulmonary Surfactant Monolayer and Formation of Lipoprotein Corona. *ACS Nano* **2013**, *7*, 10525–10533.
42. Vlasova, I. I.; Vakhrusheva, T. V.; Sokolov, A. V.; Kostevich, V. A.; Gusev, A. A.; Gusev, S. A.; Melnikova, V. I.; Lobach, A. S. PEGylated Single-Walled Carbon Nanotubes Activate Neutrophils to Increase Production of Hypochlorous Acid, the Oxidant Capable of Degrading Nanotubes. *Toxicol. Appl. Pharmacol.* **2012**, *264*, 131–142.
43. Bhattacharya, K.; Sacchetti, C.; El-Sayed, R.; Fornara, A.; Kotchey, G. P.; Gaugler, J. A.; Star, A.; Bottini, M.; Fadeel, B. Enzymatic 'Stripping' and Degradation of PEGylated Carbon Nanotubes. *Nanoscale* **2014**, *6*, 14686–14690.